

PULSE WIDTH MODULATED IGBT AC CHOPPER

Mátyás HUNYÁR and Károly VESZPRÉMI

Department of Electrical Machines and Drives
Budapest University of Technology and Economics
H-1521 Budapest, Hungary

Received: July 5, 2000

Abstract

A new circuit is presented for three-phase voltage controller (AC chopper) constructed from IGBTs. Traditionally such an equipment contains thyristors as switching elements. All drawbacks of this solution come from its only possible control method: firing control. The new circuit allows Pulse Width Modulation (PWM) control, providing much better properties. A new and advantageous control method is presented, including the protections also. Many application fields can be found, all require AC voltage control. The examined ones are: Energy-saving control of induction motor drive; Compensation of an unbalanced supply; Active filtering of the upper harmonics; Excitation system of brushless motor.

Keywords: AC chopper, IGBT, PWM, Over-current protection, energy-saving, compensation of unbalanced supply, brushless excitation.

1. Introduction

Voltage controllers are increasingly applied as motor soft starters and sometimes as energy savers, reducing the flux level in the connected induction motor in accordance with the load [1, 2, 3]. However, the use of a practical SCR voltage controller results in considerable harmonic distortion and substantial additional losses which reduce the net energy saving. The use of PWM AC chopper eliminates partially this drawback. Nowadays the applied bi-directional switches may consist of two IGBTs and diodes connected to each other in opposite direction (inverse series connection, see *Fig. 1*). For proper control, the short-circuit of the supply and breaking the motor current must be avoided.

2. Analysis

In the case of proper control, the on and off periods occur in the three phases simultaneously, and the number of chopping periods during one cycle of the line voltage is assumed to be an integer multiple of six (i.e. $6n$). The locus of the voltage Park-vector is assumed to be symmetrical with respect to the three phase axes for the sake of simplicity of calculations (see *Fig. 2*).

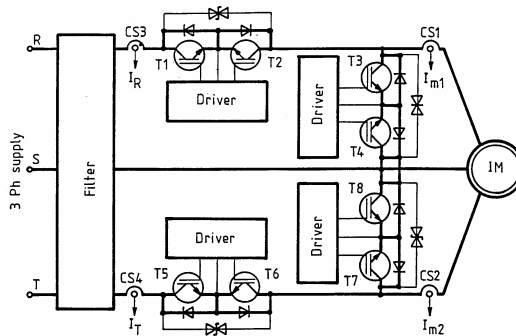


Fig. 1. Circuit diagram of the PWM AC chopper

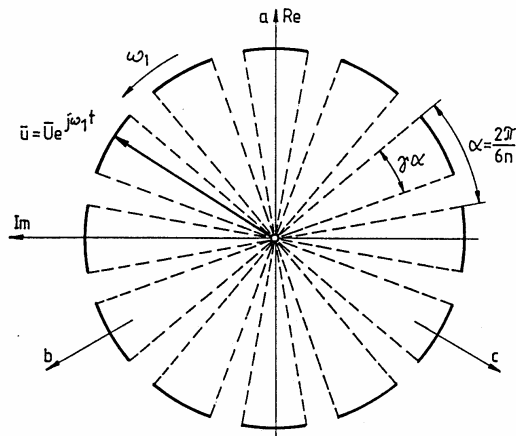


Fig. 2. Locus of the terminal voltage Park-vector

Excluding the lowest chopping frequency (i.e. $n \leq 2$) the largest deviation from the fundamental current can be approximated as

$$\Delta i_{\max} = \pm I_{\text{sci}}(1 - \gamma) \sin \frac{\pi}{6n} \gamma, \quad (1)$$

where γ is the duty cycle, I_{sci} is the ideal short-circuit current of the motor.

Note that Δi_{\max} is independent of the actual load of the motor.

For high chopping frequencies the extreme value occurs for the duty cycle of $\gamma = 0.5$. In Fig. 3 the largest values of $|\Delta \bar{i}| = \Delta i_{\max}$ are shown for different pulse numbers.

The deviation of the instantaneous current from the fundamental component $\Delta \bar{i} = \bar{i} - \bar{I}_1$ has almost exactly the same direction as the instantaneous supply

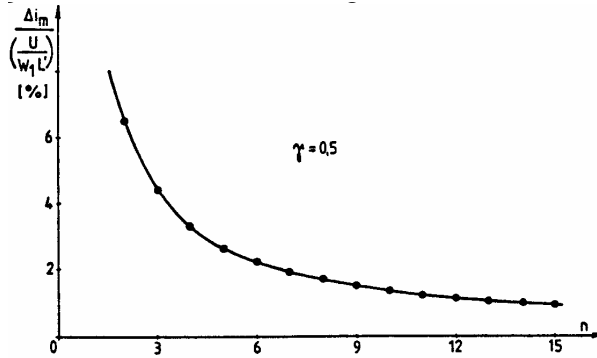


Fig. 3. The largest deviation of the instantaneous current from its fundamental vs. ‘ n ’

voltage Park-vector. Applying the projection rule of space vectors, the envelope curves of the instantaneous ‘ a ’ phase current are:

$$(i_a)_{\text{env.}} = I_1 \sin(x - \varphi_1) \pm \Delta i_{\text{max}} \cdot \sin x, \quad (2)$$

where $x = \omega_1 t$ is the rotational angle of the fundamentals, and φ_1 is the phase angle of the fundamental current. The time functions are demonstrated for $\varphi_1 = 30^\circ$ in Fig. 4.

In the time interval $x_2 - x_1$ the instantaneous phase current changes its sign several times depending on the chopping frequency.

From Fig. 4 it is evident, that the actual values of Δi_{max} in the vicinity of the zero transition of the fundamental current are function of the phase angle φ_1 , so in optimum case an adaptive current band would be required applying the control method proposed in [3] (but at very high chopping frequency it is not necessary). Regarding the distortion the duration of $x_2 - x_1$ interval is the best characteristic. Solving Eq. (2) for zero transition:

$$\text{tg } x_{1,2} = \frac{I_1 \sin \varphi_1}{I_1 \cos \varphi_1 \pm \Delta i_{\text{max}}}. \quad (3)$$

3. The Proposed Triggering Signal Logic

This control method [4] does not distinguish between the ‘normal operation’ and the zero crossing states of the motor currents. It always performs the same switching cycles that only depend on four input signals, namely the signs of the motor currents (I_{m1} ; I_{m2}) the chopper control signal U_c (on/off) and the ENABLE command.

The proposed control method allows zero transition of current in both directions, and in both cases, when the series and when the parallel switches are conducting (see Fig. 5).

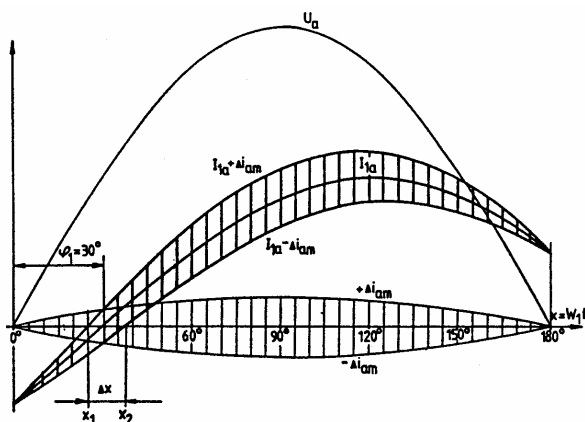


Fig. 4. The envelope curves of the instantaneous phase current vs. time

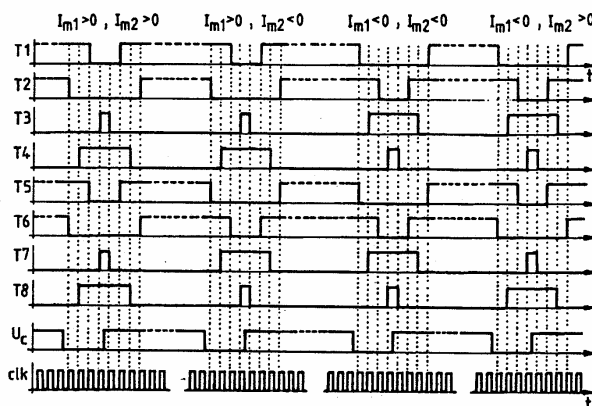


Fig. 5. The different switching sequences depending on the sign of motor line currents

In contrast to the literature, the present control theory does not regard the three-phase AC chopper as two single-phase ones operating independently. The on and off states occur simultaneously in the three-phases. The over-current protection, acting by means of deactivating the ENABLE signal, operates the similar switches in the two lines. Either current sign changes, the switching sequence will be determined by another path of the flow-chart (see Fig. 6).

The proper triggering method avoids:

- Breaking the inductive motor current, which causes over-voltage.
- Short-circuiting the supply, even for a really short time. The input filter

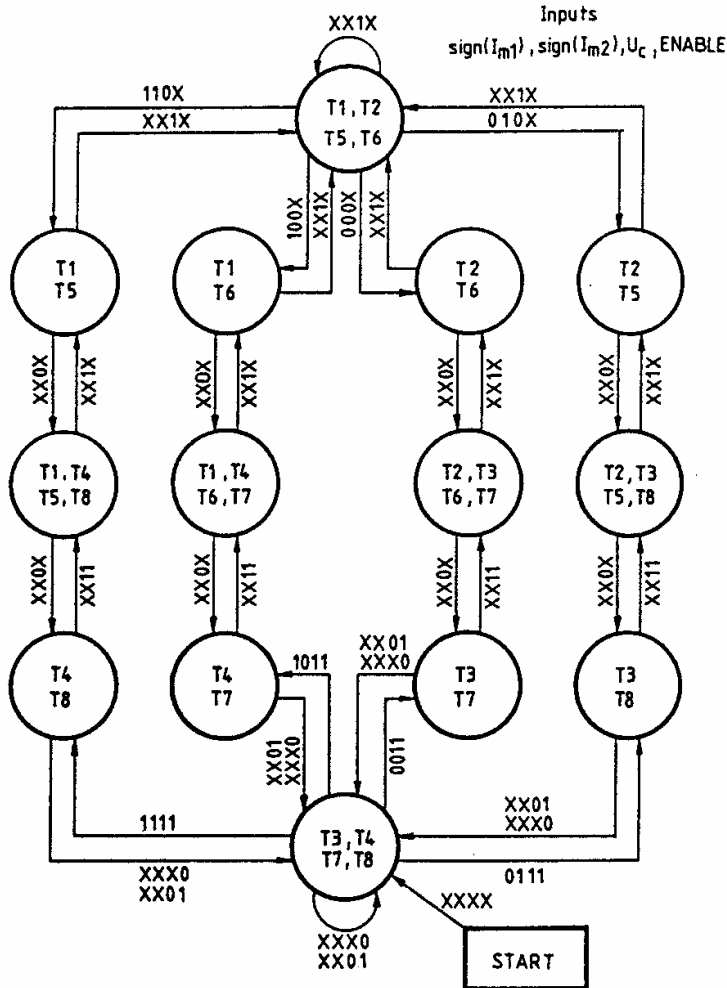


Fig. 6. Flow-chart for the triggering signal logic

contains series inductances and parallel capacitances. The capacitances are on the chopper side, providing better voltage source supply, not allowing the overlap of the series and parallel conducting.

In Fig. 5 four possible switching sequences are demonstrated according to the signs of I_{m1} and I_{m2} . The switching events are initiated by the rising edge of the first clock signal after the change of the level of control signal U_c . The frequency of the clock signal is 1 MHz. Firstly the unnecessary switch (determined by the actual current sign) is turned off. Secondly the required oncoming transistor

is triggered on. Then the previously conducting element is switched off, finally the complementary transistor of the actually conducting one is turned on, providing alternative paths for the current. The above mentioned proper switching sequence is implemented by means of a synchronous-sequential circuit. The chopper control signal U_c is a square-wave with maximum 4.5 kHz frequency (so $n = 15$). The output parameters are the gating signals of the eight IGBT-s, which are fed to the gate driver circuits via D-latches. The synchronous-sequential circuit itself is realized with an EPROM circuit feedbacked with D-latches. Six of the output signals are sufficient for feedback. The EPROM is addressed by ten signals.

In the flow-chart (Fig. 6) the marks of the actually conducting elements, and the actual input signals can be seen.

3.1. Test Results

The recorded results [5] slightly differ from the ideal ones. It can be identified mainly in the voltage Park-vector loci, where at the switching instant other transients occur than in the ideal case. It is not possible to reduce the inductance of the power circuit to zero. To reduce the effect of the slight residual stray inductance small capacitances are connected across the IGBTs. These LC elements cause the distortion of the voltage Park-vector loci at the switching instants. These are the lines from the outer 'circle' to the origin, but they have negligible effect on the fundamental harmonic of the resultant voltage. The presented figures are recorded with such a supply voltage which contains considerable 5th and 7th upper harmonics.

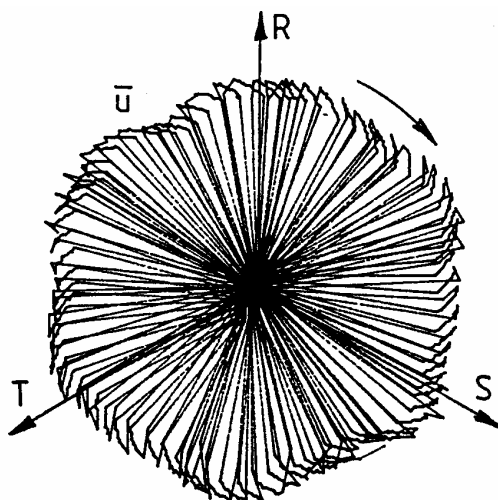


Fig. 7. Motor voltage for 0.5 duty cycle

The recorded results can be seen in *Figs. 7* and *8*. Both of them are recorded for 0.5 duty cycle, to see the effect of the largest ripple of the quantities.

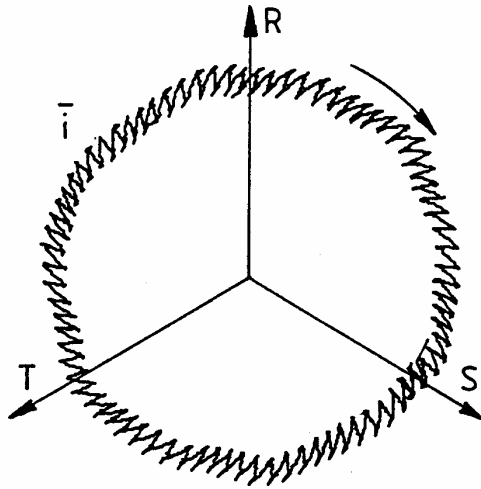


Fig. 8. Motor current for 0.5 duty cycle

4. Current Sensing and Over-Current Protection

The sensed current signals are used for the following purposes in this drive:

- over-current protection,
- feedback signal for current and other control purposes,
- proper gating control.

The three applications have different requirements.

The over-current protection of the IGBTs may not be individual not to interrupt the motor phase current. This protection acts via the input signal ENABLE. Then the switching events are performed in the proper sequence according to *Fig. 5* and *Fig. 6*. After maximum three clock period ($3\mu\text{s}$) the series switches start to turn off. Finally all the series switches are opened and all the parallel switches are closed. The current sensors (CS3, CS4 in *Fig. 1*) for over-current protection have to be placed in series with the series IGBTs to sense the accidental short circuit of both the main circuit outputs and the parallel IGBTs. The components have to be very fast (the resultant delay time may not be longer than $1.5\mu\text{s}$).

4.1. Simulation of the Long $\overline{U} = 0$ State

Short-circuiting the terminals of the motor for a long time, high over-current can be expected. One part of the magnetic energy stored in the motor is dissipated on the stator resistance. The step change in the motor terminal voltage results in a high current on the relatively small stator resistance. This way of the over-current protection causes also an over-current, which can be higher than the protection level, destroying the power switches.

To investigate this over-current during this process, simulations have been performed [6]. For qualitative analysis sinusoidal supply can be applied. The same operating point is investigated as in the other later simulations and test results ($w_{sl} = 2\%$ slip frequency).

The peak value of the current vector is approximately 5 pu which is surely beyond the protection level. The time interval during which the current magnitude is larger than 1 pu is approximately 20 ms.

It is not an acceptable shut-down procedure of this drive! Instead, the power circuit and the triggering logic are modified slightly: Surge absorbers with U_z clamping voltages are connected across each line of the motor, allowing the turn off the parallel switches also in the case of shut-down.

4.2. Selection of the U_z Clamping Voltage

Two values will determine the necessary clamping voltage of the surge absorbers: the maximum of the motor current and the consumed energy by these components during the shut-down process. These two values are calculated as the function of U_z . These curves are presented in Fig. 9.

The consumed (dissipated) energy on the surge absorbers (E) depends on two factors: the time interval necessary for reaching zero current and the instantaneous value of the power. The longer this time interval, the larger the decreasing in the flux level during the process, so the larger the magnetic energy to be dissipated in the stator circuit. Increasing the voltage U_z , this time interval is reduced significantly, and a decrease can be expected in the dissipated energy on the surge absorbers (larger energy is dissipated in the rotor). It can be seen beyond $U_z = 0.3$ pu clamping voltage. There is a maximum in this energy at 0.3 pu clamping voltage, which can be understood from an opposite increasing tendency.

The other examined value i_{\max} , the maximum of the motor current is obviously decreasing with the increasing clamping voltage. Beyond a load dependent value in U_z , no over-current is generated, since the clamping voltage is high enough to decrease the current immediately.

$U_z > 0.6$ results in no over-current and small dissipated energy on the surge absorbers.

It is better to select $U_z > U_n$, which does not require additional switches. It needs only bi-directional voltage clamping devices. Of course, the U_z clamping

voltage must be selected carefully. There is a lower limit for this, determined by the maximum supply voltage of the operation with good safety. The higher limit is determined by the allowable maximum voltage of the semiconductors. The clamping device must be fast enough to satisfy the dynamic requirement.

In this way the power circuit is simple. Between every line a bi-directional clamping device is connected.

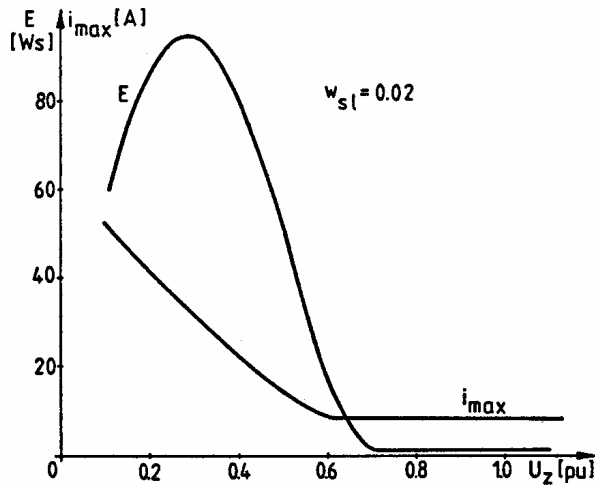


Fig. 9. The effect of the different U_z clamping voltages

4.3. Test Results

With the selected clamping device ($U_z = 1.2$ pu) measurements have been recorded on the experimental drive. The voltage and the current space vector loci are recorded for a switching off process from the full voltage (Fig. 10). The current is decreased to zero fast, as expected with this large clamping voltage. On the voltage space vector locus only one side of the constant clamped line voltage hexagon can be seen. The supply voltage contains relatively large 5th and 7th harmonics.

4.4. Current Sensing for Feedback and for Proper Triggering

The current sensors (CS1, CS2) for these purposes have to be placed in series with the motor phases behind the parallel switches.

Inserting inverse-parallel diodes into the two controlled motor phases, the detection of the actual current directions becomes possible down to very small

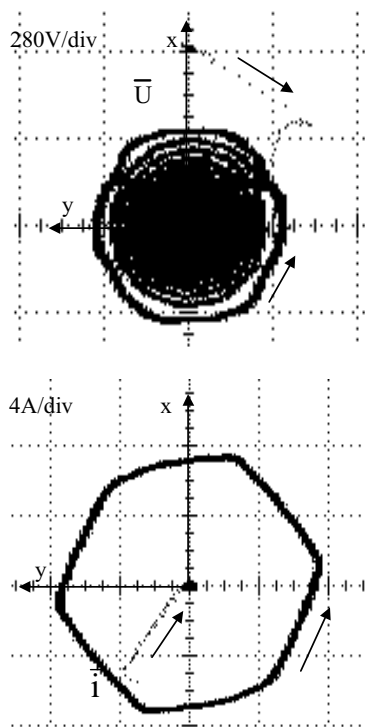


Fig. 10. The recorded space vector loci

magnitudes, (10 mA) and with very high speed ($\leq 0.5 \mu\text{s}$). In the low power range the use of Schottky diodes moderates the amount of the extra losses caused by this mode of current sign sensing.

The input filter is an inherent part of the circuit which provides nearly a voltage source feeding for the chopper circuit, as well as provides the line EMI filtering.

5. Application Fields

5.1. Energy Saving Control

The first application of the PWM AC chopper – induction motor drive is dedicated to energy-saving operation and soft starting. The operation with minimum power loss can easily be realized by means of motor terminal impedance control with subordinated current loop (Fig. 11). The constant part (Z_{1REF}^*) and the load dependent parts (Z_{NL1} , Z_{NL2}) of the impedance reference signal (Z_{1REF}) are set according to the predetermined optimal characteristic.

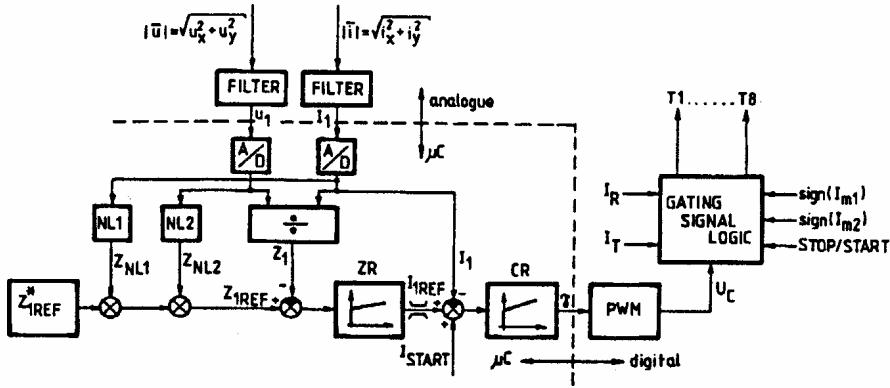


Fig. 11. Control circuit of energy-saving operation

Dividing the voltage U_1 with the current I_1 , the actual impedance signal Z_1 valid for fundamentals is obtained. The impedance controller ZR and current controller CR set the required duty cycle for the digital pulse width modulator (PWM). Then it controls the gating signal logic by means of the control signal U_C .

The operation of the drive is controlled by a microcomputer based on TMS32010 digital signal processor (DSP). It provides high computing power for the necessary calculations.

The total control algorithm is implemented in software with U_1, I_1, Z_{1REF}^* input signals, providing the output signal for PWM.

5.1.1. Comparing the SCR and the PWM Voltage Controllers

Considering energy saving, the SCR voltage controller is not a counterpart of an IGBT PWM AC chopper. To demonstrate the difference, measurements are performed by thyristor and by IGBT PWM AC chopper. The same load torque is $M = 11.2 \text{ Nm}$, which is not the best to emphasise the advantage of the PWM chopper.

Adjusting the fundamental voltage of the motor, Fig. 12 can be recorded for the motor losses (P_l), for the reactive power (Q) and for the effective current (I_{effm}).

5.1.2. Inverter or Chopper?

For constant speed drives a question is emerging: inverter or AC chopper. If the drive starts frequently or the required starting torque is high, the inverter is more attractive, providing large starting torque and low starting losses. If the drive is

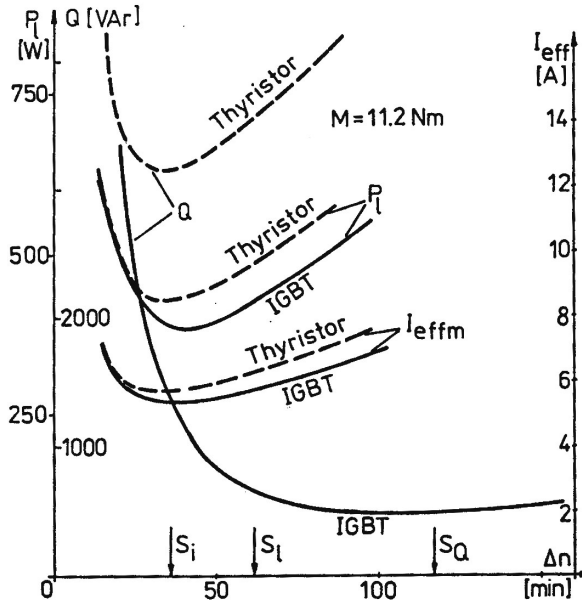


Fig. 12. Performance comparison of the SCR and the IGBT AC chopper

starting rarely, the AC chopper can be applied. For a drive, which cannot be sorted to the above discussed two categories, particular investigation must be done.

Motor Losses

Assuming the above mentioned energy-saving control method for both power circuits, the motor fundamental losses are the same, only the harmonic losses must be examined. Of course, the fundamental frequency is 50 Hz for both drives.

Calculation Method

To calculate the harmonic losses, the harmonic voltages and the harmonic currents must be determined. For comparison the switching frequency of the experimental drives must be considered. The smallest 2.9 kHz provides the best displayable result.

For this switching frequency, the calculated harmonic losses in the motor (rotor P_{Rv} and total P_{lv}) are presented in Fig. 13 as a function of the pu load torque. The chopper causes the greatest harmonic loss at 0.5 duty cycle (approximately 0.14 pu torque). Below 0.2 pu torque in the example, the chopper generates more harmonic losses, but beyond this load it is much better than the inverter supply. The two drives are designed to reach the maximum voltage at 0.62 pu torque with the optimal energy-saving control. From this point, for the inverter the harmonic loss is constant (and maximum) and for the chopper it is zero.

To make a decision, which power circuit to select, one has to know operating time ratio between the operation below and above approx. 0.2 pu torque.

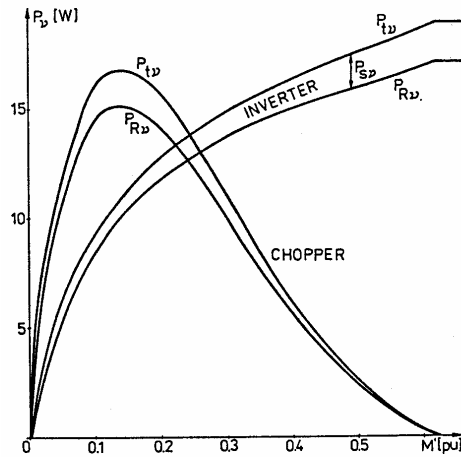


Fig. 13. Comparison of the harmonic losses of the motor

5.2. Voltage Stabilizer; Compensation of Unbalanced System

Unbalanced voltage system has significant effect on the loads extremely on the induction machines. This machine is considerably sensitive to voltage system unbalance. Traditionally the unbalanced supply of this machine can be examined by the symmetrical components method. The zero sequence component is not considered, since the stator winding of the induction motors is either delta-connected or isolated star-connected. The negative sequence current in the machine caused by the unbalanced voltage can be surprisingly large, because of the low negative sequence impedance, less than or at least equal to the short-circuit impedance of the machine. The most critical effect of the negative sequence currents is the considerable additional losses generated even at a few percent unbalance.

If the reason of the supply unbalance cannot be avoided, the nominal power of the machine must be de-rated (or reversely, for a given required mechanical power, an oversized machine is necessary). Above 5% relative unbalance the operation of an induction machine is not recommended from that supply.

5.2.1. Compensation of the Supply Unbalance

Above the 5% relative unbalance, or if the magnitude of the unbalance is varying and its reason cannot be avoided, it is advisable to use additional equipment to compensate the unbalance. In the case of higher power network, supplying more loads, the series compensation is recommended having smaller rated power (see later).

If the compensation should be done for one motor, especially if its soft starting and over-current protection also must be provided, it is advisable to use a voltage controller, inserted between the supply and the load transferring the total power. By this method the voltage can only be decreased. If the load requires the nominal voltage of the network, a transformer is necessary between the supply and the equipment. To decrease the rated power of the transformer, auto-transformer is recommended to be used.

5.2.2. SCR Voltage Controller

Traditional way is the SCR voltage controller consisting of inverse-parallel thyristors. In this case to compensate the unbalance the phases must be controlled independently. The known disadvantage of this method is that it generates small order harmonics with significant magnitudes, and its control is complicated. Less known is, however, that the ability of this method to compensate the unbalance is limited. It is demonstrated in *Fig. 14* how is possible to compensate an unbalanced voltage system [8].

5.2.3. Implementation of the Compensation by IGBT Voltage Controller

By the PWM IGBT chopper better performance can be expected. On the one hand, the orders of the generated harmonics are shifted to the larger ones determined by the switching frequency. On the other hand, more simple control can be realized. In this case, the compensation of the voltage unbalance can be done by the control of the voltage vector magnitude. The mean value of the load voltage in the switching period can be controlled by the duty cycle.

The applied chopper can control constant average voltage magnitude in every switching period. The control principle and the implementation are very simple: sensing the voltage Park-vector of the supply or the load, according to the desired voltage magnitude the necessary PWM duty cycle can be calculated in every switching period [8].

Control Methods

The strategy of the control can be different for different purposes. The common part of the controls is the inner voltage regulation/control. The intervention can be done by the γ duty cycle. It can be calculated in two ways:

Closed loop control: Processing the error signal calculated from the reference signal and the voltage magnitude of the load by a (fast) PI controller, its output is γ .

Open loop control: From the desired voltage magnitude (U_{ref}) and the sensed supply voltage magnitude (U) γ can be calculated directly: $\gamma = U_{\text{ref}}/U$.

The voltage magnitude used for the control is calculated from the Park-vector components: $U = \sqrt{u_x^2 + u_y^2}$. The closed loop control needs the voltage of the load, but it cannot be used directly for this purpose because of the PWM control, a filter effect should be implemented somehow.

Filtering the Sensed Voltage Magnitude

The mean value of the load voltage for the switching cycle is necessary for accurate control. One method to provide it is an analogue filtering of the Park-vector magnitude. Since it inherently generates a phase lag, thus not an instantaneous value is sampled, this method cannot be used.

Instead of the hardware implementation of the filter let's apply the ability of the software to calculate really the mean value of the load voltage for the switching cycle. The magnitude of the supply voltage must be sensed (U). From the actual γ duty cycle the feedback signal used by the closed loop controller can be calculated by the following expression: $U_m = \gamma U$.

Test Results

A significant artificial unbalance of the three-phase supply voltage was generated (by a single-phase transformer) for the measurements. The network itself is not sinusoidal, containing significant 5th and 7th (supply transformer saturation) harmonics.

The closed loop control was used for the measurements. To decrease the effect of the dead-time caused by the sampling, linear estimation of the sensed voltage is used. One time function was recorded without estimation to demonstrate the effectiveness of the estimation (3'). The Park-vector components of the output voltage contain the switching harmonics, so they are not suitable directly to demonstrate the operation of the compensation. Filtering the switching harmonics for both components by second order filters, the mean value of the vector for the switching cycles can be displayed. The voltage Park-vector loci (*Fig. 15*) and the time functions of their magnitude (*Fig. 16*) are recorded for four voltage references.

Recording the outer locus marked by 1 the reference signal was so high that the duty cycle of the chopper was 100%, so this curve represents the Park-vector locus of the supply. For the other reference signals the desired voltage magnitude was always below the magnitude of the supply voltage in the whole period. Either from the Park-vector loci or from the time functions the proper quality of the constant magnitude control is visible, but the angular speed of the vector along its locus is not. Of course, the angle of the vector cannot be controlled by the constant magnitude control method, the existing unequal running caused by the unbalance and by the harmonics cannot be compensated (*Table 1*).

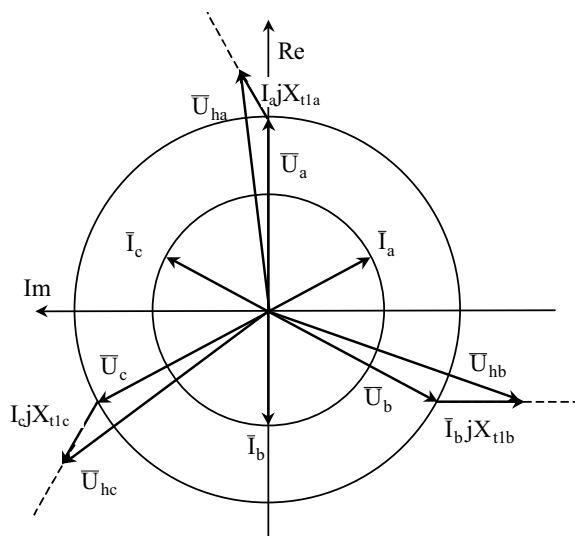


Fig. 14. Compensation by SCR voltage controller

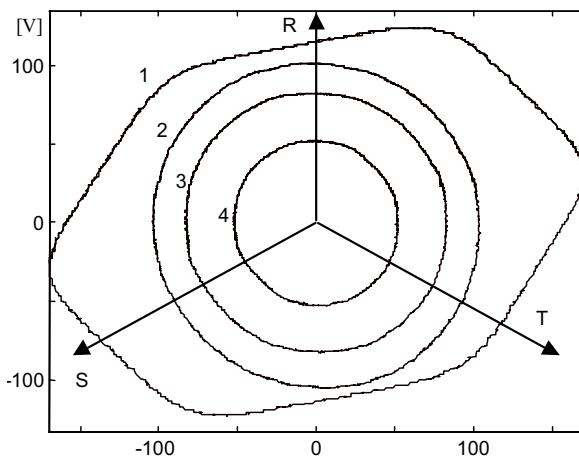


Fig. 15. The compensated Park-vector loci

It is visible that the control for constant magnitude shifts the harmonics towards higher orders (the 5th and the 7th are decreased significantly). The negative sequence component is decreased to its half approximately (it cannot be compensated perfectly) and 3rd harmonic is generated instead.

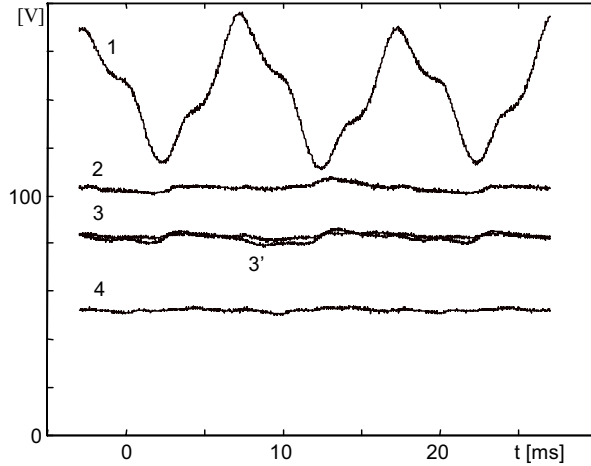


Fig. 16. The compensated voltage vector magnitudes vs. time

Table 1. Qualitative analysis of the measurements

No	U_1 [V]	U_{-1}/U_1	U_3/U_1	U_5/U_1	U_7/U_1
1.	141.1	17.8%	0.09%	2.81%	1.29%
2.	102.8	8.45%	8.92%	0.79%	0.65%
3.	82.3	8.71%	9.00%	0.89%	0.59%
3'.	81.8	8.10%	8.97%	0.86%	0.88%
4.	51.8	8.75%	9.34%	0.96%	0.48%

5.2.4. Improved Control Method

The negative sequence component exists in the uneven magnitude of the vector on the one hand and in its unequal angular velocity on the other. Controlling only the magnitude, not the constant magnitude control provides the best result in respect to the compensation of the negative sequence component. Generally, for setting the voltage magnitude reference, the angular velocity of the supply voltage vector must be considered. The negative sequence component can be compensated perfectly by this method in optimal case.

Simulations are performed by sinusoidal components to prove its operation. Now the actual supply contains about 7% negative sequence component. The desired magnitude is modulated according to the above description by different degree of modulation. In the direction of the smaller axis of the ellipse (locus) of the supply a larger voltage reference is necessary, the whole supply voltage is

applied there in the simulation. In the direction of the larger axis of this ellipse the reference signal is decreased step-by-step from 100% till 50%. The resulting positive and negative sequence components and 3rd harmonic are displayed vs. this degree of modulation in Fig. 17. The $|\overline{U}_m| = \text{const.}$ points (mark *) and the points corresponding to the minimal (zero) negative sequence component (mark o) are marked also. It is visible that the negative sequence component is transformed to 3rd harmonic, against which the impedance of an inductive circuit is much higher, the additional current is decreased. For practical implementation of the proposed new method the angular velocity of the supply voltage vector must be sensed.

5.3. Filtering the Upper Harmonics

The ‘improved control method’ mentioned in the previous paragraph can be suitable for the filtering of low order upper harmonics (e.g. for the 5th and 7th harmonics) with a little modification.

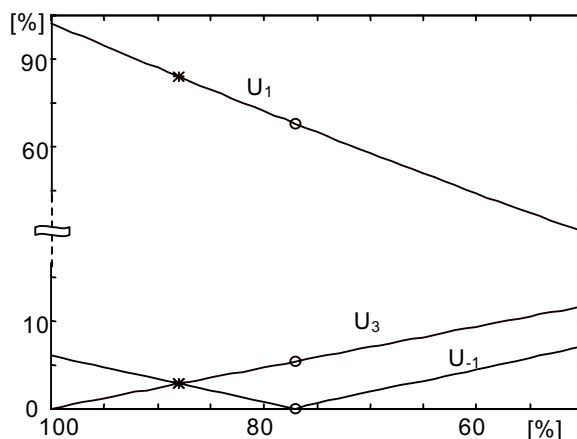


Fig. 17. Effects of the new compensation method

5.4. Series Compensation

With increasing ratings and dynamics of self-commutated semiconductor devices the use of AC chopper with PWM techniques for series compensation of power systems becomes feasible.

In contrast with VSI used for the same purpose, the IGBT (or GTO) AC chopper has the advantage of, firstly, lower harmonic content in the duty-cycle range

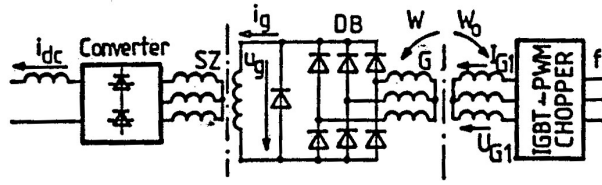


Fig. 18. Brushless excitation system of synchronous motor

of $0.5 < \gamma \leq 1$ (see Fig. 13) and, secondly, the ability of easier compensation of unbalanced power systems.

Different sophisticated schemes can be developed depending on either the magnitudes of the voltages to be controlled, or the phase angles of the voltages to be varied, or the demand might be to control both values. In all cases the additional voltages are injected in the system by series boosting transformers.

5.5. Excitation System of Brushless Motor

Recently, mainly the converter controlled synchronous motor drives (SZ in Fig. 18) were furnished with brushless excitation systems. Considering that the synchronous motor requires excitation even in standstill, a 'rotating transformer' (i.e. an induction machine with wound rotor) has to be applied (machine marked with G in Fig. 18). Traditionally the control of the field current is carried out with SCR voltage controller on the stator side of the "rotating transformer". Thus in the rotor circuit of machine G there is a current constraint and in the stator circuit there is a voltage constraint simultaneously. These cause considerable extra losses by the current and voltage higher harmonics dependent on the operating point, consequently the 'rotating transformer' has to be oversized.

By means of IGBT PWM AC chopper the extra losses can be moderated and the reactive power demand of the induction machine – AC chopper system can be reduced substantially.

Acknowledgement

This paper was supported by the Hungarian N.Sc. Fund (OTKA No. T023816 and T032207) and SIEMENS research award for which the authors express their sincere gratitude.

References

- [1] MOZDER, A. JR. – BOSE, B. K., Three-Phase AC Power Control Using Power Transistors, *IEEE Trans. Ind. Appl.*, **IA-12** (1976), pp. 499–505.
- [2] BRUNELI, B. – CASADEI, D. – SERRA, G., T-shaped LIM Driven by a Three-Phase PWM AC Chopper, In *Proceedings of the Conference EPE'91*, Florence, **I** (1991), pp. 493–498.
- [3] CASADEI, D. – GRANDI, G. – SERRA, G., Analysis of a Three-Phase PWM AC Chopper for Variable-Voltage Control of Induction Motors, In *Proceedings of the Conference ACEMP'92*, Kuşadasi, **I** (1992), pp. 744–749.
- [4] HUNYÁR, M. – SCHMIDT, I. – VESZPRÉMI, K. – MOLNÁR, T., Analysis of Control Strategy of Energy-Saving Induction Motor Drive Fed by Three-Phase PWM AC Chopper, In *Proceedings of Conference ICEM'94*, Paris, **I** (1994), pp. 257–262.
- [5] HUNYÁR, M. – SCHMIDT, I. – VESZPRÉMI, K. – MOLNÁR, T., Performance Analysis of an Energy-Saving IGBT PWM AC Chopper-Fed Induction Motor Drive Controlled by DSP, In *Proceedings of the Conference ACEMP'95*, Kuşadasi, **I** (1995), pp. 327–332.
- [6] VESZPRÉMI, K. – HUNYÁR, M. – SCHMIDT, I., Overcurrent Protection of a PWM AC Chopper-Fed Induction Motor Drive, In *Proceedings of the Conference PEMC'96*, Budapest, **3** (1996), pp. 203–207.
- [7] HUNYÁR, M. – SCHMIDT, I. – VESZPRÉMI, K. – MOLNÁR, T., Inverter or AC Chopper? – Comparative Study Concerning Energy-Saving in Induction Motor Drives, In *Proceedings of the Conference ICEM'96*, Vigo, **I** (1996), pp. 225–230.
- [8] HUNYÁR, M. – VESZPRÉMI, K., Compensation of Unbalanced Supply Voltage by Three-Phase PWM AC Chopper, In *Proceedings of the Conference CICEM'99*, Xi'an, **II** (1999), pp. 776–779.